

Bureau representation, Squier's form, and non-Abelian anyons

Alexander Kolpakov

January 27, 2026

Abstract

We introduce a frequency-tunable, two-dimensional non-Abelian control of operation order constructed from the reduced Bureau representation of the braid group B_3 , specialised at $t = e^{i\omega}$ and unitarized by Squier's Hermitian form. Coupled to two non-commuting qubit unitaries A, B , the resulting switch admits a closed expression for the single-shot Helstrom success probability and a fixed-order ceiling p_{fixed} , defining the fixed-order ceiling p_{fixed}^* and the witness gaps $\Delta_{\text{sw}}(\omega) = p_{\text{switch}}(\omega) - p_{\text{fixed}}^*$ and $\Delta_{\text{test}}(\omega) = p_{\text{test}}(\omega) - p_{\text{fixed}}^*$.

The non-Abelian mixers can either enhance or suppress the bare switch advantage, which we quantify by the interference contrast $\Delta_{\text{int}}(\omega) := \Delta_{\text{test}}(\omega) - \Delta_{\text{sw}}(\omega) = p_{\text{test}}(\omega) - p_{\text{switch}}(\omega)$. Across the Squier positivity region, $\Delta_{\text{int}}(\omega)$ takes both positive (constructive) and negative (destructive) values, a hallmark of matrix-valued (non-Abelian) order control, while $\Delta_{\text{sw}}(\omega) > 0$ certifies algebraic causal non-separability.

Numerical simulations confirm both enhancement and suppression regimes, establishing a minimal B_3 braid control that reproduces the characteristic interference pattern expected from a *Gedankenexperiment* in anyonic statistics.

1 Introduction

Indefinite causal order (ICO) is typically modeled by the *quantum switch*- a coherent superposition of two operation orders, AB and BA [1, 2]. Most cer-

tifications of ICO employ the *process-matrix* framework and causal witnesses formulated as semidefinite programs (SDPs) [3, 4].

While there are frameworks [4–7] for indefinite causal order that involve three observers – commonly known as Alice, Bob, and Charlie – only two operations are coherently superposed in order. Thus, even though three parties appear, the algebraic structure remains that of a single “swap-order” generator, effectively equivalent to the braid group $B_2 \simeq \mathbb{Z}$. By contrast, the minimal non-Abelian braid group B_3 has two independent generators σ_1, σ_2 obeying the Yang–Baxter relation $\sigma_1\sigma_2\sigma_1 = \sigma_2\sigma_1\sigma_2$, and admits non-trivial two-dimensional unitary representations that are *matrix*- rather than *phase*-valued, marking the transition from Abelian order interference to genuine non-Abelian braiding.

Recent theoretical and experimental works have begun to explore braiding phenomena in non-Abelian or non-Hermitian contexts, including three-band acoustic lattices [8], non-Abelian photonic braid monopoles [9], and programmable photonic lattices for non-Abelian topology [10]. These studies realize eigenvalue braids or non-unitary transfer operators in parameter space, but they do not address the explicit B_3 representation acting unitarily on a two-dimensional control space.

Here we introduce a representation-theoretic model of coherent order control based on the reduced Burau representation $\psi(w)$ of B_3 , specialized at $t = e^{i\omega}$ and rendered unitary by Squier’s Hermitian form [11, 12].

Within this framework, the control mixer $M(\omega)$ is a 2×2 unitary obtained from a braid word w , and the overall switch combines two non-commuting target operations $A, B \in U(2)$ through a controlled superposition of orders. The resulting process $T(\omega)$ admits closed-form discrimination probabilities through Helstrom’s theorem [13], allowing us to define two witness gaps $\Delta_{\text{sw}}(\omega)$ (bare switch) and $\Delta_{\text{test}}(\omega)$ (with mixers), and the derived *interference contrast* $\Delta_{\text{int}}(\omega) := \Delta_{\text{test}}(\omega) - \Delta_{\text{sw}}(\omega)$. Here $\Delta_{\text{sw}}(\omega) > 0$ certifies causal non-separability, while the sign of $\Delta_{\text{int}}(\omega)$ distinguishes constructive from destructive non-Abelian modulation of the two causal orders.

Unlike B_2 -based or non-Hermitian constructions, the present formulation yields a minimal, fully unitary B_3 -based *Gedankenexperiment* in which non-commuting braid generators couple directly to non-commuting target operations. This establishes a concrete mathematical route by which non-Abelian exchange statistics could be detected through order-sensitive interference.

2 Manuscript contents

Section 3 sets up the Burau–Squier control and the switch. Section 6 defines the task and discusses the Helstrom formula. Section 7 contains the main theorem: closed-form witness constructed from the braid group, while the reproducible code is available on GitHub [14].

3 Braid group control and the switch

Let $V \cong \mathbb{C}^2$ and $A, B \in U(2)$ with $[A, B] \neq 0$. The control space, as usual, is $C = \mathbb{C}^2$ with basis $\{|0\rangle, |1\rangle\}$.

Braid group on three strands. Let B_3 denote the braid group on 3 strands. There are several equivalent definitions of this mathematical object.

Topological / combinatorial. B_3 is the group of ambient isotopy classes of geometric 3–strand braids in the cylinder $D^2 \times [0, 1]$, with group law given by vertical concatenation (stacking). Cf. [15, 16].

Abstract group presentation. B_3 is generated by elementary crossings σ_1, σ_2 subject to the Yang–Baxter relation

$$B_3 \cong \langle \sigma_1, \sigma_2 \mid \sigma_1 \sigma_2 \sigma_1 = \sigma_2 \sigma_1 \sigma_2 \rangle. \quad (1)$$

Mapping class group. $B_3 \cong \text{MCG}(D^2 \setminus \{3 \text{ marked points}\})$, the mapping class group of a thrice-punctured disc where braids are represented as motions of punctures (or mutually distinguishable marked point) with time [15].

Pictures. The generators and a sample word are depicted in Figure 1: black curves are strands; time flows upward. We place strand 1 on the left, 2 in the middle, and 3 on the right. Thus, the picture of σ_1 , resp. σ_2 , is the positive crossing of strands (1, 2), resp. (2, 3).

Reduced Burau representation for B_3 . For $w \in B_3$ and a parameter $t \in \mathbb{C} \setminus \{0\}$, the reduced Burau representation

$$\psi : B_3 \longrightarrow \text{GL}(2, \mathbb{Z}[t, t^{-1}])$$

is defined on generators by

$$\psi(\sigma_1) = \begin{pmatrix} -t & 1 \\ 0 & 1 \end{pmatrix}, \quad \psi(\sigma_2) = \begin{pmatrix} 1 & 0 \\ t & -t \end{pmatrix}, \quad (2)$$

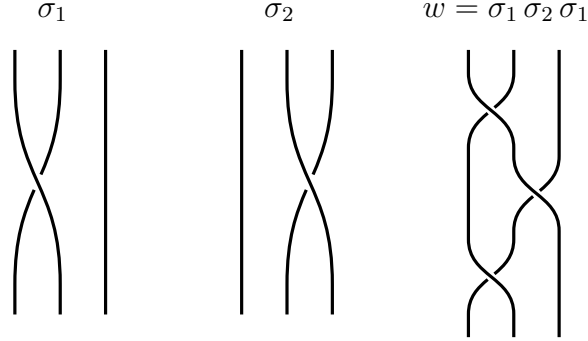


Figure 1: Two braid generators of B_3 , σ_1 and σ_2 , and their product $w = \sigma_1 \sigma_2 \sigma_1$ (which satisfies $w = \sigma_2 \sigma_1 \sigma_2$, up to strand rearrangement).

and extended by way of homomorphism:

$$\psi(\sigma_{i_1} \sigma_{i_2} \dots \sigma_{i_k}) = \psi(\sigma_{i_1}) \psi(\sigma_{i_2}) \dots \psi(\sigma_{i_k}). \quad (3)$$

The generators given above are the standard 2×2 reduced Burau matrices; see [15, § 3] or [16, § 3.1].

Faithfulness for B_3 . The reduced Burau representation can be defined for any $n \geq 2$, and is known to be *faithful* (i.e. a group isomorphism) for $n \leq 3$ [16, § 3.3.2]; by contrast, it is not faithful for $n \geq 5$ [17–19]. For $n = 4$, it is still an open problem. In general, braid groups are known to be *linear*, i.e. they admit a faithful linear representation [20, 21]. However, this representation does not have its image inside $\text{GL}(2)$.

4 Squier’s unitarization

Let s be an indeterminate with involution $\bar{s} = s^{-1}$ and set $t = s^2$. Squier’s modification of the reduced Burau representation is the homomorphism

$$\beta : B_3 \longrightarrow \text{GL}(2, \mathbb{Z}[s, s^{-1}]), \quad \sigma_i \longmapsto \beta_i = \beta(\sigma_i),$$

defined on generators by

$$\beta_1 = \beta(\sigma_1) = \begin{pmatrix} -s^2 & s \\ 0 & 1 \end{pmatrix}, \quad \beta_2 = \beta(\sigma_2) = \begin{pmatrix} 1 & 0 \\ s & -s^2 \end{pmatrix}. \quad (4)$$

On the coefficient ring $\mathbb{Z}[s, s^{-1}]$ we use the $*$ -involution given by entry-wise $\bar{\cdot}$ and transpose: $M^* := \overline{M}^T$, with $\bar{s} = s^{-1}$.

Squier exhibits the Hermitian form

$$J(s) = (s + s^{-1}) I_2 - \begin{pmatrix} 0 & 1 \\ 1 & 0 \end{pmatrix} = \begin{pmatrix} s + s^{-1} & -1 \\ -1 & s + s^{-1} \end{pmatrix}, \quad (5)$$

and proves the identities

$$\beta_i(s)^* J(s) \beta_i(s) = J(s) \quad (i = 1, 2). \quad (6)$$

After specialization $s = e^{i\omega/2}$, and hence $t = s^2 = e^{i\omega}$, equation (6) gives us ordinary $J(\omega)$ -unitarity.

Relation to the standard reduced Burau. Let us set

$$D(s) = \text{diag}(1, s^{-1}).$$

Then

$$\psi(\sigma_i) = D(s)^{-1} \beta(\sigma_i) D(s), \quad \tilde{J}(s) = D(s)^* J(s) D(s), \quad (7)$$

and consequently $\psi(\sigma_i)^* \tilde{J}(s) \psi(\sigma_i) = \tilde{J}(s)$.

Unitary specializations and the control parameter. We regard ω as a phase parameter defined modulo 2π , and fix the representative

$$\omega \in [0, 2\pi). \quad (8)$$

Specializing at $s = e^{i\omega/2}$ (hence $t = s^2 = e^{i\omega}$), the Squier form becomes

$$J(\omega) = \begin{pmatrix} 2 \cos(\omega/2) & -1 \\ -1 & 2 \cos(\omega/2) \end{pmatrix}. \quad (9)$$

Its eigenvalues are $\lambda_{\pm}(\omega) = 2 \cos(\omega/2) \mp 1$, and thus

$$\det J(\omega) = 4 \cos^2(\omega/2) - 1. \quad (10)$$

Consequently, $J(\omega) \succ 0$ holds precisely on the open set

$$\Omega_+ = (0, 2\pi/3) \cup (4\pi/3, 2\pi), \quad (11)$$

with boundary points $\omega \in \{0, 2\pi/3, 4\pi/3\}$ corresponding to $\det J(\omega) = 0$. By the symmetry $\omega \mapsto 2\pi - \omega$ of (10), we shall restrict to $\omega \in (0, 2\pi/3)$ in our numerical experiments.

On any connected component of Ω_+ where $J(\omega) \succ 0$, choose the Cholesky factor $J(\omega) = R(\omega)^\dagger R(\omega)$. For any braid word $w \in B_3$ we define the Euclidean-unitary specialization by the similarity transform

$$U(\omega) := R(\omega) \beta(w) \Big|_{s=e^{i\omega/2}} R(\omega)^{-1} \in U(2), \quad (12)$$

which is unitary because $\beta(w)^\dagger J(\omega) \beta(w) = J(\omega)$.

4.1 Positivity window, pseudo-unitarity, and roots of unity

The identities (6) imply that, for every ω , the specialized matrices $\beta_i(\omega) := \beta_i \Big|_{s=e^{i\omega/2}}$ preserve the Hermitian form $J(\omega)$ in the sense $\beta_i(\omega)^\dagger J(\omega) \beta_i(\omega) = J(\omega)$. The additional condition $J(\omega) \succ 0$ is only needed to convert this *J-unitarity* into an ordinary *Euclidean* unitarity on a two-dimensional control qubit by writing $J(\omega) = R(\omega)^\dagger R(\omega)$ and conjugating as in (12). Outside the positivity region Ω_+ in (11), the form $J(\omega)$ has mixed signature (one positive and one negative eigenvalue), so the same matrices are naturally *pseudo-unitary* (with respect to an indefinite inner product), rather than elements of $U(2)$.

Relation to roots-of-unity truncations in braided Majorana-qubit models. In the braided Majorana-qubit framework of Toppan [22, 23], roots of unity play a different operational role: they label truncations (organized into “levels”) of multi-particle sectors in a braided Hopf-algebra construction. Those works argue that, within that setting, certain inequivalent physics classes depend only on the primitive roots-of-unity structure of $t = e^{i\omega}$. By contrast, the present study investigates a two-dimensional *control* representation obtained by unitarizing the reduced Burau representation via a positive Hermitian form $J(\omega)$. In this operational model, only the subset $\omega \in \Omega_+$ yields an ordinary $U(2)$ control mixer; Galois-conjugate choices of t may therefore land in distinct branches (Euclidean-unitary versus pseudo-unitary) when viewed through the Squier unitarization. This does not contradict roots-of-unity equivalences in the multi-particle braided-Majorana setting:

our “positivity window” is the condition for realizing the control as an honest qubit unitary in (12).

Boundary points. At the boundary values $\omega \in \{0, 2\pi/3, 4\pi/3\}$ one has $\det J(\omega) = 0$ and the Cholesky-based conjugation becomes singular; while the specialized Squier matrices may satisfy additional finite-order relations at such roots of unity [22, 23], these boundary points do not define a standard Hilbert-space unitary control via (12). Thus, we shall not pursue investigating these special cases either.

5 Switch block and test device

Given ω such that $J(\omega) \succ 0$ and $J(\omega) = R(\omega)^\dagger R(\omega)$, set

$$M(\omega) := U(\omega), \quad (13)$$

where $U(\omega)$ is defined in (12) for the chosen braid word $w \in B_3$.

Define the switch as

$$S(\theta) = |0\rangle\langle 0| \otimes BA + e^{i\theta} |1\rangle\langle 1| \otimes AB, \quad (14)$$

where $\theta = \theta(\omega)$ is an arbitrary phase map.

The full test device is

$$T(\omega) = \left(M_{\text{post}}(\omega) \otimes I \right) S(\theta(\omega)) \left(M_{\text{pre}}(\omega) \otimes I \right), \quad (15)$$

where we allow distinct braid words to produce $M_{\text{pre}}(\omega)$ and $M_{\text{post}}(\omega)$.

Lemma 5.1 (Squier positivity intervals). *For any fixed braid words $w_{\text{pre/post}} \in B_3$, the set*

$$\Omega_+ := \{ \omega \in [0, 2\pi) : J(\omega) \succ 0 \}$$

is a finite union of open intervals whose endpoints lie in Z . On each connected component $I \subset \Omega_+$ one can choose $R(\omega)$ with $J(\omega) = R(\omega)^\dagger R(\omega)$ that depends real-analytically on ω , and consequently

$$M_{\text{pre}}(\omega) = R(\omega) \beta(w_{\text{pre}}) \Big|_{s=e^{i\omega/2}} R(\omega)^{-1},$$

$$M_{\text{post}}(\omega) = R(\omega) \beta(w_{\text{post}}) \Big|_{s=e^{i\omega/2}} R(\omega)^{-1}$$

are $U(2)$ -valued, real-analytic functions of ω on I .

Proof. $J(\omega)$ has real-analytic entries in ω , hence $\det J(\omega)$ is a real-analytic 2π -periodic function; its zero set Z is finite unless $\det J \equiv 0$ (which is not the case here). Thus Ω_+ is a finite union of open intervals with endpoints in Z . On a compact subinterval of I , the spectrum of $J(\omega)$ is uniformly bounded away from 0, so the Cholesky factor $R(\omega)$ may be chosen to be real-analytic, cf. [24, Chapter II, §6.1–6.4]. Conjugation by such a matrix $R(\omega)$ preserves analyticity, and J -unitarity of $\beta(\cdot)$ implies $M_{\text{pre/post}}(\omega) \in U(2)$. \square

Proposition 5.2 (Smoothness of the whole device). *On every positivity interval $I \subset \Omega_+$ from Lemma 5.1, the map $\omega \mapsto T(\omega)$ is real-analytic as a $U(2)$ -valued function. In particular, all matrix entries of $T(\omega)$, its eigenvalues and eigenphases, spectral projectors, and any polynomial or rational functions thereof are real-analytic in ω .*

Proof. By Lemma 5.1, $M_{\text{pre/post}}(\omega)$ are real-analytic on I . The map $\omega \mapsto e^{i\theta(\omega)}$ is smooth and real-analytic, if θ is. Hence, so is $S(\theta(\omega))$. Products of real-analytic matrix-valued functions are real-analytic. \square

6 Helstrom's formula and convexity witness

In order to determine if more than just interference of two causal orders takes place in the test device, we use single-shot binary discrimination with equal priors.

Helstrom for unitaries. Let U_0, U_1 be two unitaries. The optimal single-shot success is

$$p^*(U_0, U_1) = \frac{1}{2} \left(1 + \sin \frac{\delta}{2} \right), \quad (16)$$

where $\delta \in [0, \pi]$ is the shortest eigenphase arc (spectral spread) of $U_0^\dagger U_1$. Equation (16) follows from the Helstrom bound [13] specialized to two unitaries U_0, U_1 with equal priors.

Lemma 6.1 (Helstrom formula for unitaries). *Let $U_0, U_1 \in U(2)$ and define $V = U_0^\dagger U_1$. Let $\delta \in [0, \pi]$ be the length of the smallest closed arc on the unit circle containing the spectrum of V . Then the optimal single-shot, equal-prior success probability for distinguishing U_0 and U_1 is*

$$p^*(U_0, U_1) = \frac{1}{2} \left(1 + \sin \frac{\delta}{2} \right).$$

Proof. Since the trace norm is invariant under unitary action, distinguishing U_0 from U_1 is equivalent to distinguishing I from $V = U_0^\dagger U_1$ on some pure state $|\psi\rangle$. For equal priors, Helstrom's theorem gives

$$p^*(U_0, U_1) = \frac{1}{2} \left(1 + \frac{1}{2} \max_{|\psi\rangle} \left\| |\psi\rangle\langle\psi| - V |\psi\rangle\langle\psi| V^\dagger \right\|_1 \right).$$

For a rank-1 projector, the trace norm is computable in closed form:

$$\left\| |\psi\rangle\langle\psi| - V |\psi\rangle\langle\psi| V^\dagger \right\|_1 = 2\sqrt{1 - |\langle\psi|V|\psi\rangle|^2}.$$

Hence

$$p^*(U_0, U_1) = \frac{1}{2} \left(1 + \sqrt{1 - \rho(V)^2} \right), \quad \rho(V) := \min_{|\psi\rangle} |\langle\psi|V|\psi\rangle|.$$

Because V is unitarily diagonalisable, its *numerical range* $W(V) = \{\langle\psi|V|\psi\rangle : \|\psi\| = 1\}$ is the convex hull of its eigenvalues: all $\{e^{i\theta_k}\}$ are situated on the unit circle. The minimal modulus $\rho(V)$ is therefore the Euclidean distance from the origin to $W(V)$.

If the eigenvalues of V occupy a shortest covering arc of angular width $\delta < \pi$, then $W(V)$ is a circular arc's convex hull, and the closest point to the origin is the midpoint of the chord joining $e^{\pm i\delta/2}$, giving

$$\rho(V) = \cos(\delta/2).$$

If $\delta \geq \pi$, the convex hull contains the origin, so $\rho(V) = 0$. In either case,

$$\sqrt{1 - \rho(V)^2} = \sin(\delta/2),$$

with the convention $\sin(\delta/2) = 1$ for $\delta \geq \pi$.

Substituting back into the Helstrom expression yields

$$p^*(U_0, U_1) = \frac{1}{2} \left(1 + \sin \frac{\delta}{2} \right),$$

as claimed. □

Witness definition. Define the fixed-order ceiling

$$p_{\text{fixed}}^* := \max\{p^*(I, AB), p^*(I, BA)\}. \quad (17)$$

Define the switch and test performances

$$p_{\text{switch}}(\omega) := p^*(I \otimes I, S(\theta(\omega))), \quad p_{\text{test}}(\omega) := p^*(I \otimes I, T(\omega)). \quad (18)$$

The corresponding witness gaps are

$$\Delta_{\text{sw}}(\omega) := p_{\text{switch}}(\omega) - p_{\text{fixed}}^*, \quad \Delta_{\text{test}}(\omega) := p_{\text{test}}(\omega) - p_{\text{fixed}}^*. \quad (19)$$

We will refer to Δ_{sw} and Δ_{test} as the switch and test witness gaps, respectively.

Proposition 6.2 (Convexity witness). *Let \mathcal{F} be the set of fixed-order processes. For equal-prior discrimination,*

$$W \in \text{conv}(\mathcal{F}) \Rightarrow p^*(W) \leq \sup_{F \in \mathcal{F}} p^*(F) = p_{\text{fixed}}^*.$$

In particular, $\Delta_{\text{sw}}(\omega) > 0$ implies $S(\theta(\omega)) \notin \text{conv}(\mathcal{F})$, and $\Delta_{\text{test}}(\omega) > 0$ implies $T(\omega) \notin \text{conv}(\mathcal{F})$.

Proof. For any discrimination strategy—specified by an input state and measurement—the success probability is given by the generalized Born rule $p(W) = \langle G, W \rangle$ for some Hermitian operator G determined by the strategy. The optimal success probability

$$p^*(W) = \sup_G \langle G, W \rangle$$

is therefore the pointwise supremum of linear functionals of W , and hence convex. For a convex mixture $W = \sum_i q_i F_i$ with $F_i \in \mathcal{F}$ and $q_i \geq 0$, $\sum_i q_i = 1$, one has

$$p^*(W) \leq \sum_i q_i p^*(F_i) \leq p_{\text{fixed}}^*.$$

Thus a positive witness gap $\Delta_{\text{test}}(\omega) > 0$ implies that $T(\omega)$ cannot belong to $\text{conv}(\mathcal{F})$. \square

Interference contrast. To isolate the *net* effect of the non-Abelian mixers beyond the bare switch, we define

$$\Delta_{\text{int}}(\omega) := \Delta_{\text{test}}(\omega) - \Delta_{\text{sw}}(\omega) = p_{\text{test}}(\omega) - p_{\text{switch}}(\omega). \quad (20)$$

Thus $\Delta_{\text{int}}(\omega) > 0$ indicates constructive non-Abelian enhancement relative to the bare switch, while $\Delta_{\text{int}}(\omega) < 0$ indicates destructive non-Abelian suppression relative to the bare switch.

7 Main Results

We evaluate the Squier representation $\beta_i(s)$ of B_3 , as discussed above, for $s = e^{i\omega/2}$ and verify $J(\omega)$ -unitarity, positive-definiteness of $J(\omega)$, and Euclidean unitarity of the conjugated matrices $U(\omega) = R(\omega)\beta(w)R(\omega)^{-1}$ as defined in (12).

The control braid word is

$$w = \sigma_1^3, \quad (21)$$

although other B_3 elements will result in similar outcomes and can be implemented by using the auxiliary code available on GitHub [14].

Single-qubit rotations. Let us use the conventional $SU(2)$ rotation matrices about the x -, y -, and z -axes,

$$R_x(\theta) = \exp\left(-\frac{i}{2}\theta\sigma_x\right) = \begin{pmatrix} \cos\frac{\theta}{2} & -i\sin\frac{\theta}{2} \\ -i\sin\frac{\theta}{2} & \cos\frac{\theta}{2} \end{pmatrix}, \quad (22)$$

$$R_y(\theta) = \exp\left(-\frac{i}{2}\theta\sigma_y\right) = \begin{pmatrix} \cos\frac{\theta}{2} & -\sin\frac{\theta}{2} \\ \sin\frac{\theta}{2} & \cos\frac{\theta}{2} \end{pmatrix}, \quad (23)$$

$$R_z(\phi) = \exp\left(-\frac{i}{2}\phi\sigma_z\right) = \begin{pmatrix} e^{-i\phi/2} & 0 \\ 0 & e^{i\phi/2} \end{pmatrix}, \quad (24)$$

where σ_x , σ_y and σ_z are the Pauli matrices.

Das Gedankenexperiment. Let us set the target unitaries as

$$A = R_x(1.5), \quad B = R_z(0.75), \quad (25)$$

so that $[A, B] \neq 0$ while both remain simple $SU(2)$ rotations.

The switch phase is fixed as

$$\theta(\omega) = \omega, \quad (26)$$

while other functions can also be implemented in [14].

We restrict our consideration to one connected component of the Squier positivity window Ω_+ , as it is enough to demonstrate the desired properties of the test device $T(\omega)$.

For each $\omega \in (0, 2\pi/3)$, we compute:

1. J -unitarity errors $\|\beta_i^\dagger J \beta_i - J\|$ for $i = 1, 2$;
2. Euclidean unitarity error $\|U^\dagger U - I\|$ of the unitarized braid word;
3. the single-shot Helstrom success probabilities $p_{\text{switch}}(\omega)$ and $p_{\text{test}}(\omega)$;
4. the fixed-order ceiling $p_{\text{fixed}}^* = \max\{p^*(I, AB), p^*(I, BA)\}$.

The code performing these computations, together with reproducible figures, is publicly available on GitHub [14].

Theorem 7.1. *For the switch device $S(\theta(\omega))$ with $\theta(\omega) = \omega$ and target unitaries A, B defined above, the witness gap $\Delta_{\text{sw}}(\omega)$ is strictly positive for all $\omega \in \Omega_+$. For the full test device $T(\omega)$ with nontrivial mixers $M_{\text{pre/post}}(\omega)$, the interference contrast $\Delta_{\text{int}}(\omega) = \Delta_{\text{test}}(\omega) - \Delta_{\text{sw}}(\omega)$ takes both positive and negative values as a function of ω .*

Indeed, the two-dimensional Squier form $J(\omega)$ on B_3 is given by (9) and is positive definite precisely on Ω_+ given by (11).

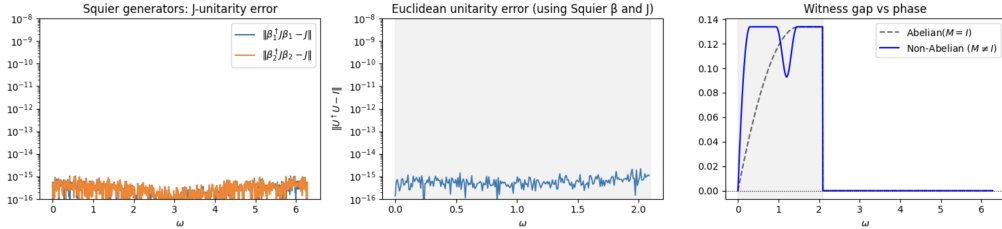


Figure 2: Left: Verification of Squier’s J -unitarity for β_1, β_2 . Center: Euclidean metric error of $U(\omega)$ within $\omega \in (0, 2\pi/3)$. Right: Witness gaps $\Delta_{\text{sw}}(\omega)$ (bare switch, Abelian control) and $\Delta_{\text{test}}(\omega)$ (with non-Abelian mixers) in the region $\omega \in (0, 2\pi/3)$. Dips of Δ_{test} below Δ_{sw} correspond to destructive non-Abelian interference, i.e. $\Delta_{\text{int}}(\omega) < 0$.

Within the window $\omega \in (0, 2\pi/3)$, the Squier generators satisfy J -unitarity to numerical precision better than 10^{-14} , and the conjugated word $U(\omega)$ is Euclidean-unitary with error $\|U^\dagger U - I\| < 10^{-14}$.

The Helstrom success for the switch exceeds the fixed-order ceiling by a gap of $\Delta_{\text{max}} \approx 0.1338$, confirming causal non-separability. An analogous statement holds for the test device.

However, in the non-Abelian test device, $\Delta_{\text{test}}(\omega)$ can exhibit pronounced *dips* relative to the bare switch gap $\Delta_{\text{sw}}(\omega)$. Equivalently, the interference contrast $\Delta_{\text{int}}(\omega) = \Delta_{\text{test}}(\omega) - \Delta_{\text{sw}}(\omega)$ becomes negative on portions of Ω_+ , signaling destructive non-Abelian interference even while $\Delta_{\text{test}}(\omega)$ may remain nonnegative.

Interpretation. The control mixer $M(\omega) \neq I$ embodies the minimal non-Abelian structure of B_3 : two non-commuting generators acting, after unitarization on Ω_+ , on a two-dimensional control space. The existence of a *positive* switch gap $\Delta_{\text{sw}}(\omega) > 0$ demonstrates that the corresponding process cannot be expressed as a convex mixture of fixed-order operations.

The existence of both constructive and destructive regimes for the *interference contrast* $\Delta_{\text{int}}(\omega) = \Delta_{\text{test}}(\omega) - \Delta_{\text{sw}}(\omega)$ draws a sharp distinction between Abelian (phase-only) and non-Abelian (matrix-valued) order control: depending on ω , the non-Abelian mixers can rotate the two order components into control subspaces that are either more distinguishable (constructive regime) or less distinguishable (destructive regime) for the optimal Helstrom measurement. This is why $\Delta_{\text{int}}(\omega)$ can change sign, thus demonstrating enhancement vs. suppression relative to the bare switch.

The non-commutativity of the braid generators is reflected in the non-commutativity of their unitarized specializations on Ω_+ , which is the defining feature of non-Abelian anyons. In the language of anyon theory, this corresponds to an effective superposition of exchange orders producing a *matrix* holonomy rather than a scalar phase.

In a hypothetical realization, each braid word w would correspond to an exchange of three distinguishable excitations, and $M(\omega)$ would represent the induced two-dimensional fusion subspace.

Hence, the present construction provides a purely algebraic *Gedankenexperiment* demonstrating how non-Abelian exchange statistics could manifest as measurable order-sensitivity, independent of microscopic substrate.

Acknowledgments

A.K. was supported by the Wolfram Institute for Computational Foundations of Science, and by the John Templeton Foundation.

References

- [1] O. Oreshkov, F. Costa, and Č. Brukner, “Quantum correlations with no causal order”, *Nature Comm.* **3**, 1092 (2012).
- [2] K. Goswami et al., “Indefinite Causal Order in a Quantum Switch”, *Phys. Rev. Letters* **121**, 090503 (2018).
- [3] M. Araújo et al., “Witnessing causal nonseparability”, *New Journal of Physics* **17**, 102001 (2015).
- [4] C. Branciard, “Witnesses of causal nonseparability: an introduction and a few case studies”, *Scientific Reports* **6**, 26018 (2016).
- [5] Y. Guo et al., *Experimental violation of a Bell-like inequality for causal order*, arXiv:2506.20516, 2025.
- [6] C. M. D. Richter et al., *Towards an Experimental Device-Independent Verification of Indefinite Causal Order*, arXiv:2506.16949, 2025.
- [7] D. Qu et al., *Experimental device-independent certification of indefinite causal order*, arXiv:2508.04643, 2025.
- [8] X. Zhang et al., “Experimental characterization of three-band braid relations in non-Hermitian acoustic lattices”, *Phys. Rev. Research* **5**, L022050 (2023).
- [9] Y. Liu et al., *Photonic Non-Abelian Braid Monopole*, arXiv:2410.08191, 2024.
- [10] H. Kim et al., *Programmable lattices for non-Abelian topological photonics and braiding*, arXiv:2410.01181, 2024.
- [11] C. C. Squier, “The Burau representation is unitary”, *Proceedings of the American Mathematical Society* **90**, 199–202 (1984).
- [12] N. Salter, “Linear-central filtrations and the image of the Burau representation”, *Geometriae Dedicata* **211**, 145–163 (2021).
- [13] C. W. Helstrom, *Quantum Detection and Estimation Theory* (1976).
- [14] A. Kolpakov, *Auxiliary code for “Burau Representation, Squier’s form, and non-Abelian anyons”*, <https://github.com/sashakolpakov/bureau-switch>, 2025.
- [15] J. S. Birman, *Braids, Links, and Mapping Class Groups*, Vol. 82, *Annals of Mathematics Studies* (Princeton University Press, 1974).

- [16] C. Kassel and V. Turaev, *Braid Groups*, Vol. 247, Graduate Texts in Mathematics (Springer, 2008).
- [17] J. A. Moody, “The Burau Representation of the Braid Group B_n is Unfaithful for Large n ”, *Bulletin of the American Mathematical Society* **25**, 379–384 (1991).
- [18] D. D. Long and M. Paton, “The Burau Representation is Not Faithful for $n \geq 6$ ”, *Topology* **32**, 439–447 (1993).
- [19] S. J. Bigelow, “The Burau Representation is Not Faithful for $n = 5$ ”, *Geometry & Topology* **3**, 397–404 (1999).
- [20] S. J. Bigelow, “Braid Groups are Linear”, *Journal of the American Mathematical Society* **14**, 471–486 (2001).
- [21] D. Krammer, “Braid Groups are Linear”, *Annals of Mathematics*, 2nd ser. **155**, 131–156 (2002).
- [22] F. Toppan, “First quantization of braided Majorana fermions”, *Nuclear Physics B* **980**, 115834 (2022).
- [23] F. Toppan, “Volichenko-type metasymmetry of braided Majorana qubits”, *Journal of Physics A: Mathematical and Theoretical* **57**, 435203 (2024).
- [24] T. Kato, *Perturbation Theory for Linear Operators*, Reprint of the 1980 Edition, *Classics in Mathematics* (Springer, Berlin, 1995).